Mutation of Arginine 121 in Lactoferrin Destabilizes Iron Binding by Disruption of Anion Binding: Crystal Structures of R121S and R121E Mutants[†,‡]

H. Rick Faber, Christina J. Baker, Catherine L. Day, John W. Tweedie, and Edward N. Baker*

Department of Biochemistry, Massey University, Palmerston North, New Zealand

Received July 15, 1996; Revised Manuscript Received September 3, 1996[⊗]

ABSTRACT: A conserved arginine residue helps to form the synergistic anion binding site in transferrins. To probe the importance of this residue for anion binding and iron binding, Arg 121 has been mutated to Ser and Glu in the N-terminal half-molecule of human lactoferrin. The two mutants, R121S and R121E, have been expressed, purified, and crystallized. Their three-dimensional structures have been determined by X-ray diffraction at 2.3 and 2.5 Å resolution, respectively. The structures were determined by molecular replacement and were refined by restrained least squares methods to final *R* values of 0.185 and 0.204. Both mutants still bind iron but with decreased stability. The crystal structures show that destabilization of iron binding probably results from disruption of the anion binding site; mutation of Arg 121 removes one wall of the anion binding pocket and causes the synergistic carbonate ion to be displaced 0.5 Å from its position in the wild-type protein. In the process it becomes partially detached from the helix N-terminus that forms the rest of the anion binding site.

Proteins of the transferrin family, typified by serum transferrin and lactoferrin, play a crucial role in controlling the levels of free iron in the body fluids of animals (Brock, 1985). In the case of transferrin, iron binding is linked with a receptor-mediated system for the delivery of transferrin-bound iron to cells (Octave *et al*., 1983). For lactoferrin, present in many external secretory fluids, no role in iron transport has been definitively established. Both proteins, however, share the ability to bind iron, as Fe^{3+}, very tightly ($K \sim 10^{20}$) but reversibly.

A unique feature of transferrin chemistry is the coupling of iron binding with the binding of a suitable anion, normally carbonate [for a review of transferrin structure and function, see Baker (1994)]. The relationship is synergistic in the sense that neither is bound tightly in the absence of the other. The nature of the binding sites and the protein conformation have been established by crystallographic studies of human lactoferrin (Anderson *et al*., 1987, 1989; Haridas *et al*., 1995), rabbit transferrin (Bailey *et al*., 1988), and chicken ovotransferrin (Kurokawa *et al.*, 1995). The molecules fold into two lobes (their N- and C-terminal halves), each with a single binding site located deep in a cleft between two similarly sized domains. The large-scale domain movement that accompanies iron binding and release has been demonstrated crystallographically in the structure of apolactoferrin (Anderson *et al.*, 1990) and by small-angle X-ray scattering (Grossmann *et al*., 1992).

The role of the anion has been proposed to be twofold: to neutralize positive charge on the protein at its binding site and to complete the iron coordination by providing two carbonate oxygen atoms as ligands (Anderson *et al.*, 1989; Baker, 1994). In so doing it bridges between the metal ion and the protein. The stability of anion binding is thus linked to the stability of iron binding, and one possible mechanism for acid-mediated iron release involves protonation of the anion and consequent destabilization of binding.

The anion binding site in the N-terminal lobe of lactoferrin is formed by residues 121−124 at the N-terminus of a helix, the side chain of Arg 121, and the side chain of Thr 117 in a preceding loop. An equivalent site is present in the C-terminal lobe of lactoferrin and in all other transferrin structures determined to date. The arginine residue is totally conserved in all transferrins, except in *Xenopus laevis* transferrin where it is changed to lysine (Moskaitis *et al.*, 1990) and in the C-terminal halves of human melanotransferrin (Rose *et al.*, 1986) and *Manduca sexta* transferrin (Bartfeld & Law, 1990) where it is changed to Ser and Thr, respectively. In the latter two cases the changes are associated (along with other mutations) with a loss of iron binding ability (Baker *et al.*, 1992). Thus all functional binding sites in transferrins appear to have a positively charged amino acid at this position.

We have examined the importance of this "essential" arginine by site-directed mutagenesis of Arg 121 in the N-terminal half-molecule of human lactoferrin (Day *et al.*, 1992a) (see Figure 1). This residue has been changed to Ser, as in the nonfunctional C-lobe site of melanotransferrin, and to Glu; the latter substitution introduces a negatively charged residue which might be expected to severely destabilize and perhaps abolish anion binding. Here we present the crystal structures of the Arg121Ser and Arg121Glu mutants and the structural and functional consequences of the mutations. The results also offer a structural explanation for the much faster iron release kinetics recently observed for Arg 124 mutants of human transferrin (Zak *et al.*, 1995).

[†] We gratefully acknowledge financial support from the Health Research Council of New Zealand, the Wellcome Trust, and the U.S. National Institutes of Health (Grant HD-20859) and from the Howard Hughes Medical Institute through an International Research Scholar's award to E.N.B.

[‡] Atomic coordinates for both structures have been deposited with the Protein Data Bank, Brookhaven National Laboratories, Upton, NY, with accession codes 1VFE (R121S mutant) and 1VFD (R121E mutant).

* To whom correspondence should be addressed (air mail). Phone: (64) (6) 350 5367. Fax: (64) (6) 350 5664. Email: T. Baker@massey.ac.nz.

[⊗] Abstract published in *Advance ACS Abstracts,* October 15, 1996.

S0006-2960(96)01729-1 CCC: $12.00 © 1996 American Chemical Society

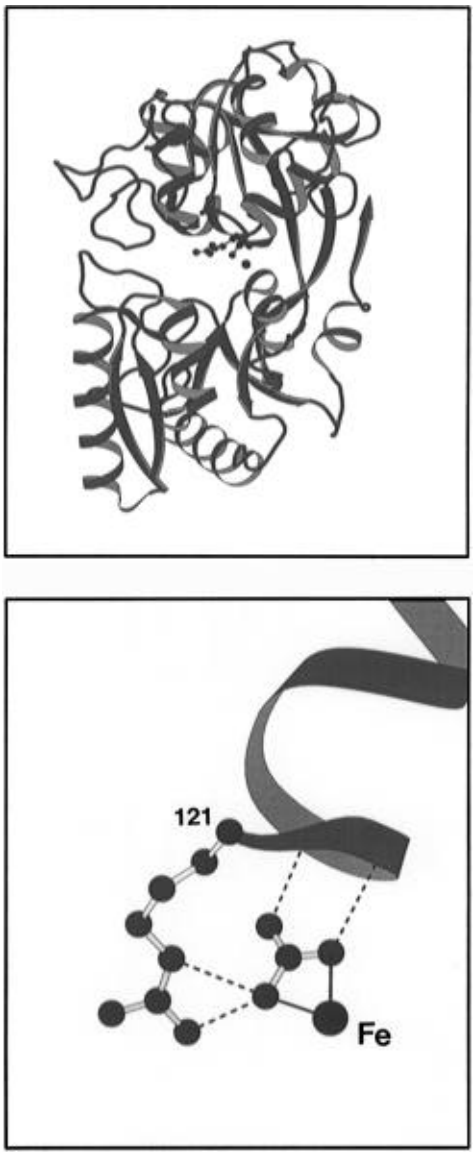

FIGURE 1: (a, top) Ribbon diagram of the lactoferrin N-terminal half-molecule, showing the location of Arg 121 and the bound Fe^{3+} and CO_3^{2-} ions, in ball-and-stick representation. Drawn with the program RIBBONS (Carson & Bugg, 1986). (b, bottom) Close-up view of the anion binding site in lactoferrin, including the role of the Arg 121 side chain. Hydrogen bonds are shown with broken lines.

MATERIALS AND METHODS

Production of Mutants. The R121S and R121E mutants were constructed and expressed using methods previously used for production of wild-type Lf_N and its D60S mutant (Day *et al.*, 1992a; Faber *et al.*, 1996). Briefly, the cDNA encoding the N-terminal half of human lactoferrin, residues 1−333, was used to prepare a uracil-containing single-strand DNA. This was used as the template for oligonucleotide-directed mutagenesis using the procedure of Kunkel *et al.* (1987) to enhance the production of mutant clones. The presence of the required mutation in individual clones was verified by DNA sequencing, and the mutant cDNA was transferred into the mammalian expression vector pNUT (Palmiter *et al.*, 1987), as described previously (Stowell *et al.*, 1991; Day *et al.*, 1992a). The pNUT:Lf_N mutant plasmid was used to transform baby hamster kidney (BHK) cells by calcium phosphate coprecipitation. Transformed cells were selected using methotrexate (0.5 mM), and expression of the mutant protein was verified by immunoprecipitation and SDS gel electrophoresis.

For large-scale production the cells were transferred into roller bottles. The mutant protein was secreted into the growth medium, which was changed daily (150 mL per day) over a period of 12−14 days. Purification from the spent growth medium was by ion-exchange chromatography (Day *et al.*, 1992a). The protein expressed in BHK cells is mostly glycosylated, at the single glycosylation site (Asn 137), but some nonglycosylated material is also produced; therefore, the protein was deglycosylated using an endoglycosidase preparation (Baker *et al.*, 1994) prior to crystallization. The yield of pure protein was in each case 10−15 mg/L of medium.

Iron Binding and Release. Before crystallization or spectroscopic studies were undertaken, sufficient 0.01 M ferric nitrilotriacetate was added to each mutant to ensure that it was fully iron saturated. Iron release, as a function of pH, was monitored by dialyzing protein samples (at a concentration of 1.5−2.0 mg/mL) in a series of buffers from pH 8.0 to pH 2.0, as described in Day *et al.* (1992a). The percent saturation at each pH was estimated by comparing the absorbance at the visible absorption maximum (454 nm for Lf_N but varying between 454 and 475 nm for the mutants) with the absorbance for the fully iron-saturated protein.

Crystallization. Both mutants were crystallized by microdialysis of concentrated protein solutions (50−60 mg/mL) against low ionic strength buffers containing a small amount of added alcohol. Crystals were obtained under essentially the same conditions for both mutants, *i.e.*, 50 mM Tris-HCl, pH 8.0, containing 12% 2-propanol.

Crystals of R121S grew as thin, orange-red plates, which were mostly heavily overgrown. For characterization and data collection, a small fragment of 0.2 × 0.1 × 0.04 mm was broken off one of the plates. The crystal was monoclinic, space group *C*2, with unit dimensions $a = 97.9$ Å, $b = 78.8$ Å, $c = 58.9$ Å, $\alpha = \gamma = 90°$, and $\beta = 99.2°$. Assuming a single molecule in the asymmetric unit, the Matthews coefficient V_M (Matthews, 1968) is 2.99 $Å^3$/Da and the solvent content 59%.

Crystals of R121E grew from an initial amorphous precipitate of the iron-saturated protein. Surprisingly, the first crystals to appear after 3−6 months were colorless hexagonal needles, apparently of the iron-free protein. Later, a small number of pale pink crystals were found. These crystals, which were used for the structure analysis, were small, flattened needles, up to 0.15 × 0.05 × 0.03 mm in size, orthorhombic, space group $C222_1$, with unit cell dimensions $a = 98.1$ Å, $b = 78.9$ Å, and $c = 113.6$ Å. Assuming one molecule in the asymmetric unit, V_M is 2.93 $Å^3$/Da and the solvent content 58%.

Data Collection. For both mutants, X-ray data collection was limited by the crystal size, which affected both the resolution and extent of the data; only one usable crystal was obtained for R121S and two for R121E. Nevertheless, the data were of surprisingly good quality. The effective resolution in each case was taken as that at which the outermost shell was ∼50% complete and had a mean I/σ ratio of at least 2.0.

For R121S, diffraction data were collected at room temperature, from a single crystal, with an R-Axis IIC image plate detector on an RU 200 rotating anode generator. Data were processed with the supplied R-Axis software (Molecular

Structure Corp.). From a total of 35 914 measurements, 14 539 unique reflections to 2.3 Å were obtained; data were 90% complete to 2.8 Å and 73.8% complete to 2.3 Å. Data in the outermost shell, 2.4−2.3 Å, were 47.5% complete, with a mean I/σ of 2.4.

For R121E, two data sets were collected from two separate crystals. The first was collected at room temperature on the R-Axis, as above, but the small size of the crystal limited the observable data to around 3 Å resolution. A second data set was collected using synchrotron data at the Photon Factory (Tsukuba, Japan); this made use of the Weissenberg camera with imaging plates (Sakabe, 1991) on beam line 6A2 with a wavelength of 1.0 Å. Data were processed with DENZO (Otwinowski, 1990). From the combined total of 44 825 measurements, 13 063 unique reflections were obtained, representing an overall completeness of 85.4%. In the outermost shell (2.59−2.5 Å) data were 57% complete, with a mean I/σ ratio of 2.0. The overall merging R was 0.081.

Structure Determination. The unit cells for the two mutants are extremely similar, differing only in the doubling of the c axis in R121E coupled with a change from monoclinic to orthorhombic symmetry. Neither is isomorphous with wild-type Lf_N crystals (Day *et al.*, 1992b), however, and the structures were therefore solved by molecular replacement. The search model was residues 5−316 of the wild-type N-lobe half-molecule, Lf_N (Day *et al.*, 1993) with the side chains of Arg 121 and the four iron ligands (Asp 60, Tyr 92, Tyr 192, His 253) all truncated to Cβ and the Fe^{3+} and CO_3^{2-} ions and all solvent molecules omitted. Rotation and translation solutions for the R121E mutant were obtained using the programs ROTFUN and FASTRAN (Zhang & Matthews, 1994); the rotation peak had a height of 6.3σ (next highest 4.4σ) and the translation peak a height of 7.5σ (next highest 4.9σ). After the molecule was positioned in the R121E unit cell, it was subjected to rigid body refinement using the program TNT (Tronrud *et al.*, 1987), first as a single rigid body and then as two separate domains, N1 (residues 5−90 + 252−316) and N2 (residues 91−251). This reduced the R-factor from 0.405 to 0.343 for 20.0−5.0 Å data. This R121E model was then used in the same way to solve the R121S mutant. Rotation and translation solutions (4.8σ and 11.8σ, respectively; next highest 3.5σ and 3.0σ) were applied, and rigid body refinement reduced the R-factor from 0.329 to 0.308.

Refinement. Refinement was by restrained least squares using the program TNT (Tronrud *et al.*, 1987) with the geometry library of Engh and Huber (1991). A subset of 10% of reflections was used to calculate the free R-factor (Brunger, 1992) as a monitor on refinement. The same strategy was used for the refinement of both mutants, involving rounds of restrained least squares refinement interspersed with checks on model geometry using PROCHECK (Laskowski *et al.*, 1993) and model rebuilding with TURBO FRODO (Roussel & Cambillau, 1991).

The initial round of refinement (with all B-factors set at 20 Å^2) reduced R to around 0.28 in each case. Missing side chains were added, including the mutated residue 121, together with Fe^{3+} and CO_3^{2-} ions. Further rounds of refinement and rebuilding, with individual isotropic B-factors assumed for all atoms, reduced R to around 0.21. At this point the placement of the CO_3^{2-} ion was reexamined through calculation of omit maps (having excluded it from the model in preceding least squares cycles). Omit map density for the CO_3^{2-} ion and the side chain of residue 121 in each mutant is shown in Figure 2. Some side chains were similarly reexamined. Solvent molecules (assumed to be water) were progressively included in the model from this point on, but following reasonably conservative criteria: a peak height of at least 3σ in $F_o - F_c$ maps and 1σ in $2F_o - F_c$ maps and favorable hydrogen bond partners and geometry. These were also reexamined by omit maps during further refinement. Density for residues 317−325 at the C-terminus could be fitted satisfactorily at a late stage in the refinement, but no clear model beyond Phe 325 or before Ser 5 could be built. Several loops were rebuilt a number of times, in particular residues 137−144 which appear to be poorly defined in all deglycosylated lactoferrin structures. The best fit for this region has Pro 142 in the *cis* configuration, as in Lf_N. The final rounds of refinement were used in rechecking the CO_3^{2-} and solvent positions and steady improvement of the protein geometry. Some statistics of the refinement are in Table 1.

Model Quality. Details of the final models are given in Table 1. Both show good agreement with the X-ray data, with final R-factors of 0.185 for R121S and 0.204 for R121E. Luzzati and σ_A plots (Luzzati, 1952; Read, 1986) are consistent with a maximum coordinate error of 0.2−0.3 Å in each structure. In both cases the model covers residues 5−325. The N-terminal residues 1−4 are poorly defined in all lactoferrin structures so far determined and here are represented by only weak, broken electron density which was not modeled. The C-terminus is also poorly ordered in these and other lactoferrin half-molecule structures (Day *et al.*, 1993; Faber *et al.*, 1996) because of the absence of the stabilizing interactions provided by the C-lobe in full-length lactoferrin; here no interpretable density was found beyond Phe 325. Several regions of the model have high B-factors, notably residues 85−87, 137−143, 162−165, and 321−325, all but the latter being highly exposed surface loops. The solvent molecules located mostly represent "core" solvent, with nearly half of them being present in both mutants and the wild-type Lf_N structure (Day *et al.*, 1993).

Ramachandran plots (Ramakrishnan & Ramachandran, 1965) show only one outlier from favored regions in each case; this is Leu 299, however, which is the central residue in a γ-turn that is conserved in all transferrin structures. Its conformational angles, (72, −59) in R121E and (63, −49) in R121S, are standard for classic γ-turns (Baker & Hubbard, 1984). Ser 191 has the ϵ configuration with angles about (70, −170). In wild-type lactoferrin Ser 191 O_γ is hydrogen bonded to Arg 121, but its conformation is unchanged here when Arg 121 is mutated, showing that it is the constraints of polypeptide folding that determine this conformation. Overall, 84.3% of the residues in R121E are in the "most favored" regions defined by Laskowski *et al.* (1993), as are 85.8% of residues in R121S.

RESULTS AND DISCUSSION

Iron Binding. Both mutants bind iron, as was shown by the red color of the proteins purified from the growth medium. The latter contains iron, and as the pH of the medium is above 7.0 during cell growth, most of the recombinant lactoferrins produced in this way are found to have iron bound. For characterization of the proteins,

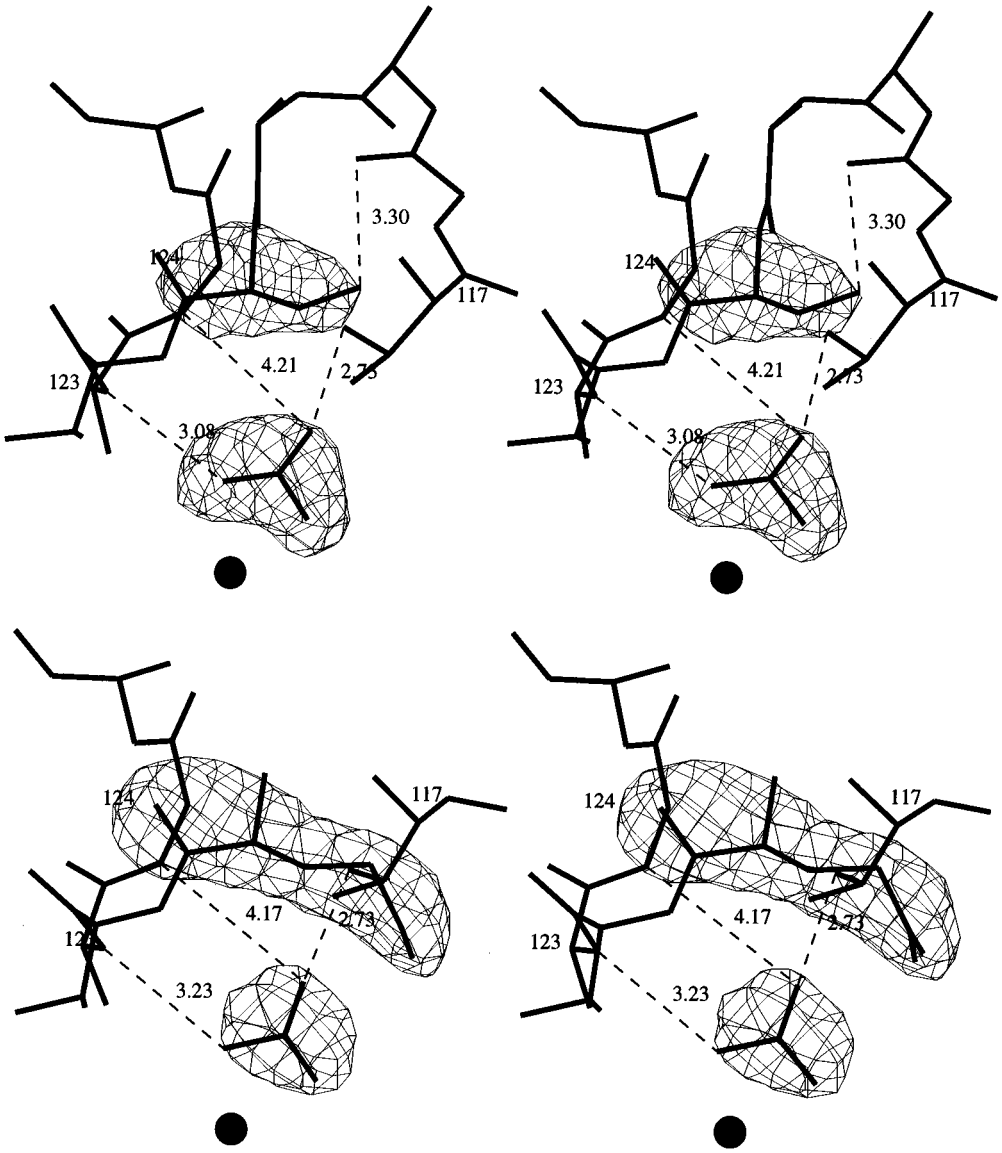

FIGURE 2: Stereo diagrams showing the final atomic model in the region around the mutation site for (a, top) the R121S mutant and (b, bottom) the R121E mutant. In each case omit electron density for the carbonate ion and the mutated residue 121 side chain is shown, contoured at a level of 5σ.

Table 1: Data Collection and Refinement Parameters

	R121S	R121E
(I) data collection		
max resolution (Å)	2.3	2.5
no. of measurements	35914	44825
no. of unqiue reflections	14539	13063
% completeness (overall)	73.8	85.4
% completeness (outer shell)	47.5 (2.3−2.4)	57.3 (2.5−2.6)
merging *R*-factor	0.086	0.081
(II) refinement		
no. of reflections used[a]	13083 (1451)	11740 (1295)
resolution range	20−2.3	20−2.5
no. of protein atoms	2496	2500
no. of solvent molecules	88	84
final *R*-factor[a]	0.185 (0.287)	0.204 (0.317)
av *B* (protein atoms) (Å^2)	22.6	35.2
av *B* (all atoms) (Å^2)	22.8	35.5
rms deviations		
bonds (Å)	0.011	0.016
angles (deg)	1.6	2.0
planes (Å)	0.017	0.020

[a] Numbers in parentheses refer to the free *R* calculation.

however, excess ferric nitrilotriacetate was added to ensure complete saturation of iron binding capacity.

Two significant differences in iron binding are found for the two mutants. First, the wavelength of maximum absorption in the visible spectrum varies when compared with the wild-type half-molecule, Lf_N. This reflects differences in the metal−ligand interactions. For the R121E mutant the change of arginine to glutamic acid causes λ_{max} to increase from 454 nm (Lf_N) to 472 nm. This parallels the red shift seen in mutants of transferrin when the formal negative charge in the binding cleft is increased (Woodworth *et al.*, 1991), although the reason for this trend is not known. For the R121S mutant, a pH-dependent change in λ_{max} is seen; at pH 8.0 λ_{max} is 454 nm, as for wild-type Lf_N, but as the pH is reduced, λ_{max} increases to around 475 nm at pH 5.5. A possible explanation for this phenomenon is that in the wild-type protein the presence of the positive charge associated with Arg 121 maintains the anion as CO_3^{2-}. However, in R121S the absence of the positive charge means that the anion is more easily protonated, forming HCO_3^-, which has different coordination properties. Whether λ_{max} for R121E is similarly pH dependent is not so easily ascertained because it does not retain iron over a sufficient pH range.

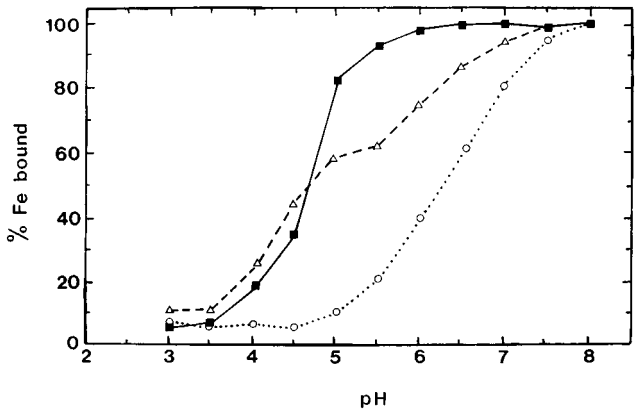

FIGURE 3: Plot comparing the pH dependence of iron release from the R121S (triangles, broken line) and R121E (circles, dotted line) mutants with that from wild-type Lf_N (squares, solid line) over the pH range 8.0−3.0.

The second difference is in the stability of iron binding. All transferrins lose iron as the pH is lowered; for wild-type Lf_N release begins at a pH around 5.5 and is complete by pH 4.0 when monitored as described here. Both mutants lose iron more readily (see Figure 3). For R121S iron release begins at pH 6.5−7.0 while for R121E it begins even higher, at a pH around 7.5−8.0. Indeed, crystallizations of the R121E mutant, at pH 8.0, produced two forms of crystal, one pink, iron saturated, and orthorhombic (the form described here) and the other colorless, iron free, and trigonal. Iron release from R121E occurs very readily below pH 7.5, being complete at pH 5.5. The shape of the pH-dependence curve for R121S is different from that of Lf_N in that although release begins at higher pH, some iron is retained to lower pH (Figure 3). The reason for this is not known.

The decreased acid stability, and more facile iron release, shown by the two Arg 121 mutants of lactoferrin parallels kinetic effects seen when the equivalent residue in transferrin, Arg 124, is mutated. Mutants of the N-terminal half-molecule of human transferrin, R124S and R124K, both show substantially faster iron release (to pyrophosphate) at pH 7.4, consistent with a critical role for the carbonate ion and the anchoring arginine side chain in stabilizing iron binding (Zak *et al.*, 1995).

Protein Conformation. Both mutants have the same overall conformation as wild-type Lf_N (Day *et al.*, 1993). In each case the molecule is folded into two domains which between them enclose the binding cleft and which are joined by two antiparallel strands of polypeptide that run behind the binding site (see Figure 1). In this respect the proteins closely resemble the bacterial periplasmic binding proteins (Quiocho, 1990) in their construction (Baker *et al.*, 1987). At the C-terminus of the half-molecule, residues 321−333 have a changed conformation from that in full-length native lactoferrin. In the latter, residues 321−332 form an α-helix, packed in the interlobe region, whereas in Lf_N residues 323−327 are extended and residues 328−333 are not visible at all and are probably disordered. In the two Arg 121 mutants the chain is only visible as far as Phe 325, residues 321−325 are neither helical nor extended as in Lf_N, and no density is seen for residues 326−333. Clearly, this C-terminal region, from Gly 321 onward, is flexible in the half-molecules and is influenced by crystal packing. Gly 321 may act as a hinge point.

Table 2: Summary of Domain Superpositions[a]

	Lf_N	R121S	R121E
Lf_N		0.38, 0.37 Å	0.43, 0.42 Å
R121S	3.5°		0.33, 0.40 Å
R121E	3.2°	0.4°	

[a] Above the diagonal are rms deviations between pairs of structures. The numbers are for the superpositions of Cα atoms of the individual domains, domain 1 followed by domain 2. Below the diagonal are differences in relative domain orientations in pairs of structures. These were obtained by superimposing on domain 1 and then seeing what rotation was required to bring the two domains 2 into register.

Superpositions of the two mutants, on each other and on Lf_N, show that the mutants are essentially identical in conformation but that they differ slightly in relative domain orientations from Lf_N. The results of these superpositions are summarized in Table 2. The two mutants differ from each other by only 0.4° in relative domain orientations, and superposition of the whole molecules (C_α of residues 5−321) gives an rms deviation comparable with those obtained for the individual domains (0.38 Å, compared with 0.33 Å for domain 1 and 0.40 Å for domain 2). When the mutants are compared with wild-type Lf_N, however, the domain orientations are found to differ by 3.5° and 3.2°, respectively, for R121S and R121E. The difference is best described as a slight twist of one domain relative to the other rather than a difference in closure such as is seen in the D60S mutant for Lf_N (Faber *et al.*, 1996).

Whether the difference in domain orientations can be attributed to the mutation is not clear. Arg 121 does lie in the interdomain cleft, and its loss could alter interactions between the domains. Moreover, the domain orientations are the same in both mutants even though they crystallize in different space groups (*C*2 and $C222_1$). On the other hand, the crystal packing is very similar for the two mutants despite the different space groups (75% of intermolecular contacts seen for R121S are also present in R121E crystals) and is different from that in Lf_N crystals. Therefore, it cannot be excluded that crystal packing may influence the relative domain orientations in these cases.

The Mutation Site. No change in protein conformation takes place around the mutation site in either mutant. Superposition of all atoms of residues 117−125 (the N-terminus of helix 5 plus the preceding loop) onto the equivalent residues in wild-type Lf_N gives rms deviations of 0.23 and 0.27 Å, respectively, for R121S and R121E. The iron binding residues, Asp 60, Tyr 92, Tyr 192, and His 253, superimpose equally well, and the only changes are in the nature and orientation of the mutated side chain.

For R121S it had been anticipated that the serine side chain could still hydrogen bond to the CO_3^{2-} anion, *i.e.*, that only the positive charge of the arginine side chain would be lost. This is not the case. Instead of hydrogen bonding to the anion, the side chain of Ser 121 folds back to hydrogen bond to the main-chain carbonyl oxygen of residue 118. Two factors account for this. First, Ser side chains have a strong preference for local hydrogen bonding, with polypeptide backbone C═O and NH groups only a few residues away. Here residues 118−121 form a type II β-turn, and a favorable rotamer ($\chi_1 = -54°$) allows the Ser side chain to hydrogen bond to the C═O of the first residue of the turn. Such side-chain $n\cdots$O ($n - 3$) interactions by Ser are common in β-turns as well as at the C-termini of helices (Baker &

Table 3: Distances in the Metal and Anion Sites

	metal−ligand bond distances (Å)				hydrogen bond distances (Å)		
	R121S	R121E	Lf_N		R121S	R121E	Lf_N
Fe−$O_{\delta 1}$(60)	2.12	1.91	1.99	O1···N_{ϵ}(121)		2.57[a]	2.90
Fe−O_{η}(92)	2.02	1.80	2.00	O1···$N_{\eta 2}$(121)			2.59
Fe−O_{η}(192)	1.74	2.03	1.92	O2···N(123)	3.08	3.23	2.81
Fe−$N_{\epsilon 2}$(253)	2.32	1.96	2.15	O3···Oγ1(117)	2.73	2.73	2.64
Fe−O1	2.04	2.12	2.09	O3···N(124)	(4.21)	(4.17)	3.31
Fe−O2	2.33	1.92	2.23				

[a] Water molecule OW519.

Hubbard, 1984). Second, this interaction would exist in the apoprotein prior to metal and anion binding and is presumably too favorable to be altered by the binding of the CO_3^{2-} ion nearby. Similar considerations apply to the D60S mutant recently analyzed (Faber *et al.*, 1996), where the mutated Ser side chain remains bound to a helix N-terminus in an $n\cdots$NH ($n + 2$) interaction rather than binding to the iron atom.

The result in the R121S mutant is that no hydrogen-bonding group, not even a water molecule, takes the place of the arginine side chain.

For R121E a possible scenario was that the introduced Glu side chain would fold back to allow its carboxyl group to associate with the N-terminus of helix 5 (residues 121−125) and thus prevent anion binding. Again, this does not occur, and the Glu side chain instead extends out into the interdomain cleft (Figure 3). Its only connection with the anion site is that a water molecule, OW 519, bridges between one carboxylate oxygen and the CO_3^{2-} anion.

Consequences for Metal and Anion Binding. The main consequences of the mutations are a disruption of the anion binding site and destabilization of iron binding. In native lactoferrin (Haridas *et al.*, 1995) and in the wild-type N-lobe half-molecule (Day *et al.*, 1993), and indeed in all transferrins so far analyzed, the arginine sidechain forms one wall of the anion binding site, folding round the CO_3^{2-} ion so that the latter is enclosed between it and the N-terminus of helix 5. This is shown for Lf_N in Figure 1b. The arginine also contributes two hydrogen bonds (from N_{ϵ} and $N_{\eta 2}$) and a favorable charge interaction. Replacement by serine removes all of these interactions. Replacement by glutamic acid removes one hydrogen bond and the positive charge interaction; one hydrogen bond remains, from a water molecule, but its contribution is probably outweighed by the unfavorable presence of the negative charge of the carboxylate so close (~3.5 Å) to the anion. Probably the only side chain that can approximate to the arginine, in its interactions, is lysine, which is found in the N-lobe of *Xenopus laevis* transferrin. A lysine side chain would be more flexible, however, and could at most provide only one hydrogen bond, factors which could explain the faster release from the R124K mutant of the human transferrin half-molecule (Zak *et al.*, 1995).

The loss of the interactions provided by the arginine is seen both in the way the anion binds and in the stability of iron binding. In both mutants the results are the same. The principal effect is that the anion is displaced 0.5 Å from its position in wild-type Lf_N, in a direction toward where the arginine had been (Figure 4). In the process it has become somewhat detached from the N-terminus of helix 5, and only two hydrogen bonds with the protein remain (Table 3); the carbonate oxygen O3, which is hydrogen bonded to the peptide NH of residue 124 in native lactoferrin, and Lf_N, is now more than 4 Å away. The position of the carbonate is unequivocal (Figure 2), and the consistency between the two mutants (Figure 4) shows that the displacement must be attributable to the loss of the arginine side chain. In both mutants the anion is still bound in bidentate mode to the iron; there are suggestions that it may be less symmetrically bound in R121S, but the resolution, particularly for R121E, is not sufficient to define the anion orientation exactly.

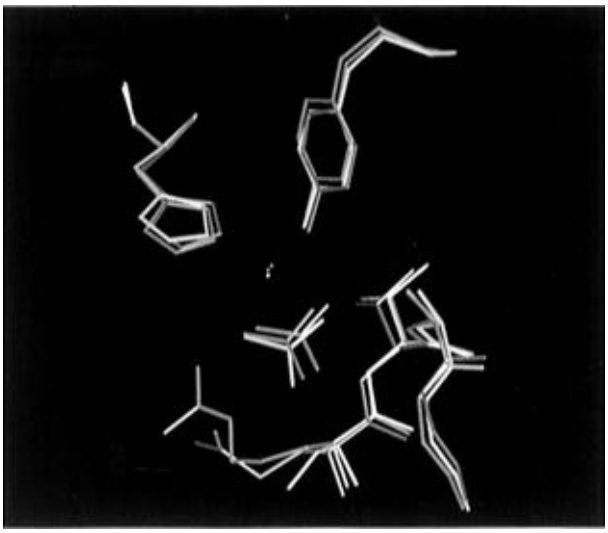

FIGURE 4: Comparison of the anion binding site in the two mutants R121S (yellow) and R121E (red) with that in wild-type Lf_N (blue). In Lf_N this is formed by the atoms of the helix N-terminus (right, bottom) and the Arg 121 side chain (left, bottom). In the mutants the CO_3^{2-} ion is displaced away from the helix N-terminus toward the position vacated by the Arg side chain.

In all other respects the iron coordination remains the same as in the native molecule and in Lf_N; the bond lengths to the four protein ligands are very similar (Table 3), and all the interdomain interactions described for Lf_N (Day *et al.*, 1993), including those contributed by Tyr 82, Arg 89, Arg 210, Glu 211, Glu 216, and Lys 301 and bound solvent molecules, are present also in the two mutants.

Our conclusion is that the weakened iron binding, seen in its more facile release, results from weakened anion binding. The same effect is seen both for lactoferrin (this work) and for transferrin (Zak *et al.*, 1995), and it emphasizes the synergistic relationship between metal and anion binding. Structurally, the loss of one wall of the anion binding site, and of the interactions contributed by the arginine, causes the anion to become partially detached from what remains of the anion site. Iron release is associated with a moving apart of the two domains (Anderson *et al.*, 1990). Since the anion forms a bridge between the metal ion and protein,

and there are relatively few interdomain interactions other than those involving the metal, any weakening of the metal−anion−protein bridge must make iron release easier. The loss of the arginine also makes the carbonate more accessible and probably more readily protonated; protonation of the carbonate at low pH would then result in decreased electrostatic attraction to the Fe(III) as suggested previously (Zak *et al.*, 1995). What this analysis also shows is that the mutation of the arginine in the C-lobes of melanotransferrin and *M. sexta* transferrin (to Ser) must be a major contributor to their loss of iron binding ability—although in itself it is not sufficient to abolish iron binding.

ACKNOWLEDGMENT

We thank Dr. N. Sakabe for help with data collection at the Photon Factory, Mr. S. C. Shewry for help with iron release measurements, Mrs. H. M. Baker for help with crystallization, and Drs. B. F. Anderson and C. A. Smith for help with data processing and preparation of figures.

REFERENCES

Anderson, B. F., Baker, H. M., Dodson, E. J., Norris, G. E., Rumball, S. V., Waters, J. M., & Baker, E. N. (1987) *Proc. Natl. Acad. Sci. U.S.A. 84*, 1769−1773.

Anderson, B. F., Baker, H. M., Norris, G. E., Rice, D. W., & Baker, E. N. (1989) *J. Mol. Biol. 209*, 711−734.

Anderson, B. F., Baker, H. M., Norris, G. E., Rumball, S. V., & Baker, E. N. (1990) *Nature 344*, 784−787.

Bailey, S., Evans, R. W., Garratt, R. C., Gorinsky, B., Hasnain, S., Horsburgh, C., Jhoti, H., Lindley, P. F., Mydin, A., Sarra, R., & Watson, J. L. (1988) *Biochemistry 27*, 5804−5812.

Baker, E. N., & Hubbard, R. E. (1984) *Prog. Biophys. Mol. Biol. 44*, 97−179.

Baker, E. N., Rumball, S. V., & Anderson, B. F. (1987) *Trends Biochem. Sci. 12*, 350−353.

Baker, E. N., Baker, H. M., Smith, C. A., Stebbins, M. R., Kahn, M., Hellström, K. E., & Hellström, I. (1992) *FEBS Lett. 298*, 215−219.

Baker, H. M., Day, C. L., Norris, G. E., & Baker, E. N. (1994) *Acta Crystallogr., Sect. D 50*, 380−384.

Bartfeld, N. S., & Law, J. H. (1990) *J. Biol. Chem. 265*, 21684−21691.

Brock, J. H. (1985) in *Metalloproteins* (Harrison, P., Ed.) Part 2, pp 183−262, Macmillan Press, London.

Day, C. L., Stowell, K. M., Baker, E. N., & Tweedie, J. W. (1992a) *J. Biol. Chem. 267*, 13857−13862.

Day, C. L., Norris, G. E., Anderson, B. F., Tweedie, J. W., & Baker, E. N. (1992b) *J. Mol. Biol. 228*, 973−974.

Day, C. L., Anderson, B. F., Tweedie, J. W., & Baker, E. N. (1993) *J. Mol. Biol. 232*, 1084−1100.

Engh, R. A., & Huber, R. (1991) *Acta Crystallogr., Sect. A 47*, 392−400.

Faber, H. R., Bland, T., Day, C. L., Norris, G. E., Tweedie, J. W., & Baker, E. N. (1996) *J. Mol. Biol. 256*, 352−363.

Grossmann, J. G., Neu, M., Pantos, E., Schwab, F. J., Evans, R. W., Townes-Andrews, E., Lindley, P. F., Appel, H., Thies, W.-G., & Hasnain, S. S. (1992) *J. Mol. Biol. 225*, 811−819.

Haridas, M., Anderson, B. F., & Baker, E. N. (1995) *Acta Crystallogr., Sect. D 51*, 629−644.

Kunkel, T. A., Roberts, J. D., & Zakour, R. A. (1987) *Methods Enzymol. 154*, 367−382.

Kurokawa, J., Mikami, B., & Hirose, M. (1995) *J. Mol. Biol. 254*, 196−207.

Laskowski, R. A., MacArthur, M. W., Moss, D. S., & Thornton, J. M. (1993) *J. Appl. Crystallogr. 26*, 283−291.

Luzzati, V. (1952) *Acta Crystallogr. 5*, 802−810.

Matthews, B. W. (1968) *J. Mol. Biol. 33*, 491−497.

Moskaitis, J. E., Pastori, R. L., & Schoenberg, D. R. (1990) *Nucleic Acids Res. 18*, 6135.

Octave, J.-N., Schneider, Y.-J., Trouet, A., & Crichton, R. R. (1983) *Trends Biochem. Sci. 8*, 217−220.

Otwinowski, Z. (1990) *DENZO Data Processing Package*, Yale University, New Haven, CT.

Palmiter, R. D., Behringer, R. R., Quaife, C. J., Maxwell, F., Maxwell, I. H., & Brinster, R. L. (1987) *Cell 50*, 435−443.

Quiocho, F. A. (1990) *Philos. Trans. R. Soc. London, Ser. B 326*, 341−351.

Ramakrishnan, C., & Ramachandran, G. N. (1965) *Biophys. J. 5*, 909−933.

Read, R. J. (1986) *Acta Crystallogr., Sect. A 42*, 140−149.

Rose, T. M., Plowman, G. D., Teplow, D. B., Dreyer, W. J., Hellström, K. E., & Brown, J. P. (1986) *Proc. Natl. Acad. Sci. U.S.A. 83*, 1261−1265.

Roussel, A., & Cambillau, C. (1991) TURBO FRODO, *Silicon Graphics Geometry Partners Directory* (Silicon Graphics, Ed.) p 86, Silicon Graphics, Mountain View, CA.

Sakabe, N. (1991) *Nucl. Instr. Methods Phys. Res. A303*, 448−463.

Stowell, K. M., Rado, T. A., Funk, W. D., & Tweedie, J. W. (1991) *Biochem. J. 276*, 349−355.

Tronrud, D. E., Ten Eyck, L. F., & Matthews, B. W. (1987) *Acta Crystallogr., Sect. A 43*, 489−501.

Woodworth, R. C., Mason, A. B., Funk, W. D., & MacGillivray, R. T. A. (1991) *Biochemistry 30*, 10824−10829.

Zak, O., Aisen, P., Crawley, J. B., Joannou, C. L., Patel, K. J., Rafiq, M., & Evans, R. W. (1995) *Biochemistry 34*, 14428−14434.

Zhang, X.-J., & Matthews, B. W. (1994) *Acta Crystallogr., Sect. D 50*, 675−686.

BI961729G